

CHARM DECAYS

SCOTT MENARY ^a

Physics Dept.

University of California

Santa Barbara, CA 93106-9530

USA

Abstract

In this paper the status of our knowledge of charm decays, both experimental and theoretical, is reviewed. The paper begins with a discussion of absolute charm branching fractions. The precision of these numbers are often the limiting factor in the unraveling of a number of issues in both charm and bottom physics. The spectroscopy of charmed hadrons continues to exhibit a rich structure and some new results on charmed baryons will be discussed. The review ends with an overview of weak decays of charmed mesons. There are more measurements on purely leptonic D_s^+ decays¹ giving a precision on the D_s^+ decay constant that is approaching the level needed to meaningfully confront a prediction of Lattice QCD. Finally, there is clearly something wrong with the current picture of either nonleptonic decays or of the constituents of η' , as will be demonstrated through a discussion of the anomalously large value of the $D_s^+ \rightarrow \eta' \rho^+$ branching fraction.

1 Introduction

The field of charm physics is at an interesting stage. There is a wealth of experimental information on mesons and baryons containing a charm quark. Yet the mass of the charm quark is such that neither of the recent theoretical advances – heavy quark symmetries and chiral perturbation theory – is really applicable. The machinery of Heavy Quark Effective Theory, which has allowed for precise comparisons of theory with experiment in the case of $b \rightarrow c$ transitions, is not as powerful when considering (not-really-)heavy-to-(not-really-)light transitions like $c \rightarrow s$.

It is difficult to make precise predictions in the charm sector because non-perturbative QCD plays such a large role in almost all charm decay physics. However, the relevant Cabibbo-Kobayashi-Maskawa (CKM) matrix elements – V_{cs} and V_{cd} – are known precisely assuming the CKM matrix is unitary. This leads to the very powerful condition that many nonperturbative quantities, like decay constants and heavy-to-light transition form factors, can be

^a Now at: Fermilab, Batavia, IL, USA

measured using charm decays and then either compared with theoretical predictions from Lattice QCD and QCD sum rules or used as input into models of b hadron decay where one wants to extract the CKM matrix elements.

Mixing and \mathcal{CP} Violation in the charm sector are predicted at levels well below present experimental sensitivity. However, many extensions of the Standard Model predict large deviations from Standard Model predictions for these phenomena making charm decays an excellent place to search for hints of such theoretical ideas.

Finally, besides allowing the study of a plethora of interesting aspects of electroweak and strong physics, charmed hadron physics is also relevant to b hadron decays since the b quark decays essentially 100% of the time to a c quark. Many of the questions concerning the weak decays of the b quark therefore require precise knowledge of the subsequent decay of the charm quark. This adds perhaps even greater motivation for measuring as many charmed hadron branching fractions as possible as well as searching for techniques to measure absolute charmed hadron branching fractions.

This is necessarily a very subjective selection of what is “important” and “interesting” in charm decay physics and I apologize beforehand for having to leave out some exciting experimental and theoretical results due to space constraints. I will not discuss rare charm decay results as they are covered elsewhere in these proceedings.² Nor will I discuss charmonium where some intriguing questions have been raised by new experimental results on both the production³ and decay⁴ of $c\bar{c}$ resonances.

2 The Experimental Players

Two experimental techniques have dominated the field of charm decay measurements – high energy beams on fixed targets and e^+e^- annihilation.

Fixed target experiments utilize some high energy beam of particles, either light quark hadrons (e.g., some mix of kaons and pions) or photons, impinging on a variety of targets. The downstream spectrometer usually contains bending magnets for measuring the momentum of charged particles, a high precision tracking system close to or including the target, some form of particle identification, and electromagnetic and hadronic calorimetry. For example, Fermilab experiment E687 collides a photon beam of $\langle E \rangle = 220$ GeV on a Be target. The large $c\bar{c}$ cross-section of $\sim\mu\text{barn}$ leads to sizable data samples even in relatively short runs. E687 wrote some 510 million events to tape. A silicon vertex detector system is used to reconstruct the secondary vertices from long-lived charmed hadrons and the ability to distinguish these vertices from the primary interaction vertex results in huge gains in signal to noise.

An event showing two fully reconstructed neutral D meson decays is shown in Figure 1. They also achieve good $K - \pi$ separation with threshold Čerenkov counters. Their results are culled from $\sim 10^5$ fully reconstructed charmed hadrons (predominantly in all charged final states).

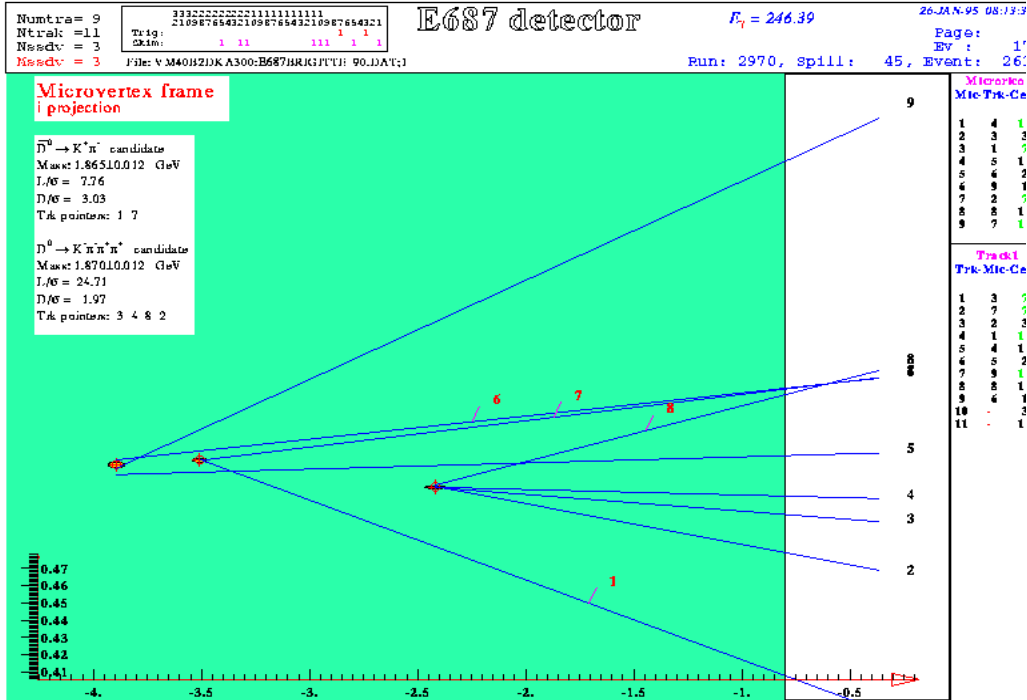


Figure 1: A fully reconstructed $D^0 - \bar{D}^0$ pair event from Fermilab experiment E687. See http://da831.fnal.gov/spectrometer/event_displays/evdisp.html for more information on this and other selected events.

In Fermilab experiment E653 the beam consists of 600 GeV π^- 's. An active emulsion target in conjunction with a silicon detector system is used for precision vertexing and allowed E653 to accumulate a small sample of charmed hadron decays with very little background.

An experiment more specific to charmed baryon physics is CERN WA89 which utilized a 330 GeV Σ^- beam impinging on a Cu/C target. Six hundred million events were recorded over 3 running periods (91/93/94). The spectrometer contained 29 planes of silicon for secondary vertex reconstruction and a RICH giving good $K - \pi$ separation up to $p = 100$ GeV/c.

The dominant experiment at e^+e^- colliders is the CLEO experiment at the Cornell Electron Storage Ring (CESR). At CESR, the highest luminosity collider in the world, the electron and positron beam energies are set to perform physics in the region of the Υ resonances, the system of $b\bar{b}$ bound states. The hadronic e^+e^- cross-section in this center-of-mass region is shown in Fig. 2. All the Υ resonances lower in mass than the $\Upsilon(4S)$ are below threshold for

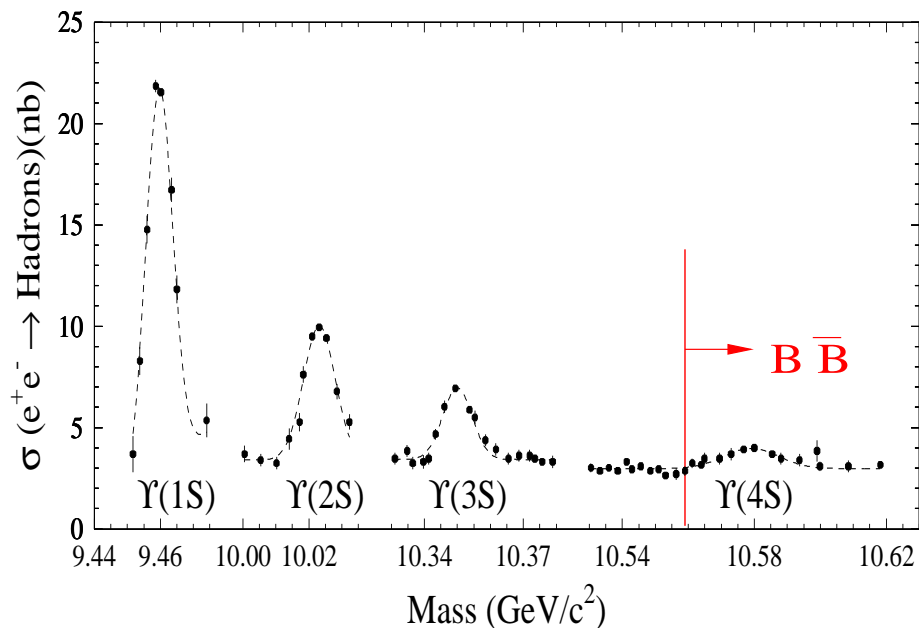


Figure 2: The $e^+e^- \rightarrow \text{Hadrons}$ cross-section in the Υ mass region.

producing a $B\bar{B}$ pair. The $\Upsilon(4S)$ cross-section is about a nanobarn above the “continuum” cross-section of ~ 3.4 nb, and $c\bar{c}$ production constitutes about a nanobarn of the continuum. Hence, every fb^{-1} of data taken at the $\Upsilon(4S)$ contains about 10^6 $B\bar{B}$ and $c\bar{c}$ pairs. Further, the b quark decays essentially 100% of the time to a c quark giving another million charmed particles per fb^{-1} . CLEO-II has recorded 3.2 fb^{-1} of data at the $\Upsilon(4S)$ and 1.6 fb^{-1} below $B\bar{B}$ threshold corresponding to ~ 10 million directly produced charmed hadrons on tape and another 6.5 million or so from the decays of B mesons. The CsI calorimeter allows the reconstruction of photons and, hence π^0 and η mesons through their decay to $\gamma\gamma$, with excellent resolution and efficiency. A silicon vertex detector was installed in CLEO in late 1995. No results from the ~ 2

fb^{-1} taken with this detector have yet been reported.

In $e^+e^- \rightarrow c\bar{c}$ events at 10.58 GeV center-of-mass, the charmed hadron carries most of the charmed quark's energy (which is the beam energy). Conversely, the absolute kinematic cutoff for charmed hadrons from B decay is $m_B/2 \approx 2.5$ GeV. This is illustrated by the inclusive D_s^+ momentum spectrum in Fig. 3 where there is a clear demarcation in momentum between D_s^+ mesons produced in B decay and those from the continuum. Since the combinatorial

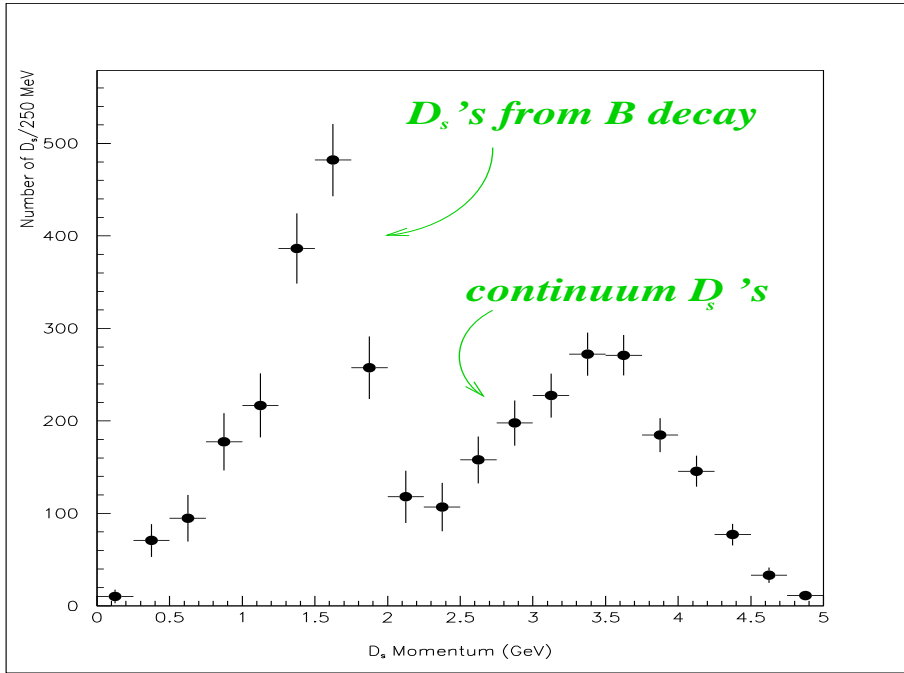


Figure 3: The CLEO-II D_s^+ momentum spectrum.

background generally falls sharply with increasing momentum, most charm analyses require a minimum charmed hadron candidate momentum of 2.5 to 3 GeV or, equivalently, $x > 0.5 - 0.6$ where $x \equiv p/p_{max}$ with $p_{max} = \sqrt{E_{beam}^2 - m_{hadron}^2}$.

3 Absolute Branching Fractions

3.1 $\mathcal{B}(D_s^+ \rightarrow \phi\pi^+)$ – Making the Waters Murkier around an Uncertain Anchor

Most charmed hadron branching fractions are given with respect to a normalizing mode. In the D sector, $D^0 \rightarrow K^-\pi^+$ and $D^+ \rightarrow K^-\pi^+\pi^+$ serve as those modes and their branching fractions are listed in the 1996 Particle Data Group Review of Particle Physics⁵ (PDG96) as $(3.83 \pm 0.12)\%$ and $(9.1 \pm 0.6)\%$, respectively. These averages are dominated by CLEO-II measurements.

What about the D_s^+ ? The PDG94⁶ value for $\mathcal{B}(D_s^+ \rightarrow \phi\pi^+)$ was $(3.5 \pm 0.4)\%$ and this 11% error dominates the systematic error for many measurements involving D_s^+ mesons. This value was derived using assumptions concerning the relationship between the D and D_s^+ semileptonic widths. There has always been some contention as to the validity of these assumptions leading to the moniker “uncertain anchor” for this branching fraction.

CLEO-II has made a new, model independent measurement⁷ of this branching fraction using, of all things, $B^0 \rightarrow D_s^{*+}D^{*-}$ decays! The technique, which originated with the ARGUS experiment and has been refined by CLEO, exploits the fact, unique to B meson production from $\Upsilon(4S)$ decays at rest, that the B meson energy is equal to the precisely measured beam energy. Consider the $B^0 \rightarrow D_s^{*+}D^{*-}$ decay chain with the D_s^{*+} and D^{*-} subsequently decaying to $D_s^+\gamma$ and $\bar{D}^0\pi^-$, respectively. Sixteen numbers are required to completely specify the decay, namely the 4-momenta of the D_s^+ , \bar{D}^0 , γ , and π^- . Let us say that one measures the \bar{D}^0 and π^- momenta as well as the γ energy. The masses of these three particles are known, thereby completely specifying their 4-momenta and leaving four unknowns. The beauty of this particular decay chain is that there are enough further constraints – specifically, $m(D_s^{*+})$, $m(\bar{D}^{*-})$, $m(B^0)$, and $E(B^0) = E(\text{beam})$ are known – that the number of $B^0 \rightarrow D_s^{*+}D^{*-}$ decays (call this $N[B \rightarrow D_s^*D^*]$) can be determined without reconstructing the D_s^+ at all! Note that this only works for vector charmed mesons like these with natural widths which are negligible on the scale of the detector resolution. $N[B \rightarrow D_s^*D^*]$ can also be determined using a fully reconstructed D_s^{*+} and just the “soft” π^- from the $D^{*-} \rightarrow \bar{D}^0\pi^-$ decay. Equating these two determinations of $N[B \rightarrow D_s^*D^*]$ then relates $\mathcal{B}(D_s^+ \rightarrow \phi\pi^+)$ to $\mathcal{B}(D^0 \rightarrow K^-\pi^+)$. A nice feature of this technique is that nearly all experimental systematic errors cancel including the relatively large reconstruction efficiency uncertainties for both the slow pion and the photon. The major systematic uncertainties are in the signal and background shapes.

The value found by this technique is $\mathcal{B}(D_s^+ \rightarrow \phi\pi^+) = (3.59 \pm 0.77 \pm 0.48)\%$ where the first error is statistical and the second is the systematic

error. Because there is no theoretical uncertainty associated with this new determination of $\mathcal{B}(D_s^+ \rightarrow \phi\pi^+)$, this value of $(3.6 \pm 0.9)\%$ is what you will find in PDG96. In other words, this new determination of $\mathcal{B}(D_s^+ \rightarrow \phi\pi^+)$ had the curious effect of *substantially increasing* the error on a branching fraction in the Particle Data Booklet. Another interesting feature of this measurement is that the D_s^+ absolute branching scale is now directly related to the value of $\mathcal{B}(D^0 \rightarrow K^-\pi^+)$, just as is case for the D^+ . This puts a premium on having as many independent measurements of the crucial $D^0 \rightarrow K^-\pi^+$ branching fraction as possible.

Finally, the physics community is still in need of some clever technique(s) for extracting absolute branching fractions in the charmed baryon sector.

3.2 The D^* Branching Fractions – Electromagnetic vs Strong Interactions

The Q value in $D^* \rightarrow D$ transitions is such that electromagnetic decay widths are comparable to strong decay widths, as evidenced by the D^{*0} branching fractions:

$$\begin{aligned}\mathcal{B}(D^{*0} \rightarrow D^0\pi^0) &= (61.9 \pm 2.9)\% \\ \mathcal{B}(D^{*0} \rightarrow D^0\gamma) &= (38.1 \mp 2.9)\%\end{aligned}$$

The D^{*+} branching fractions have an interesting history. MARK III originally measured ⁸ $\mathcal{B}(D^{*+} \rightarrow D^+\gamma) = (17 \pm 5 \pm 5)\%$, a result which seemed anomalously high. That is, in magnetic dipole (M1) decays of a $c\bar{q}$ meson, like $D^* \rightarrow D\gamma$, the decay rate in a simple potential model is proportional to $|(\mu_c + \mu_{\bar{q}})|^2$ ($= |(\mu_c - \mu_q)|^2$) where μ_q is the magnetic moment of the constituent quark q . The magnetic moment of the quark is related to the mass by $\mu_q \propto e_q/m_q$ so, assuming “reasonable” values for the quark masses $m_u = m_d = 300$ MeV and $m_c = 1500$ MeV, one would expect: ¹¹

$$\frac{\Gamma(D^{*+} \rightarrow D^+\gamma)}{\Gamma(D^{*0} \rightarrow D^0\gamma)} \approx 0.05$$

In 1992, CLEO published ⁹ the result $\mathcal{B}(D^{*+} \rightarrow D^+\gamma) = (1.1 \pm 1.4 \pm 1.6)\%$ or $< 4.2\%$ @90% C.L. and the D^{*+} branching fractions settled down to:

$$\begin{aligned}\mathcal{B}(D^{*+} \rightarrow D^0\pi^+) &= (68.3 \pm 1.4)\% \\ \mathcal{B}(D^{*+} \rightarrow D^+\pi^0) &= (30.6 \pm 2.5)\% \\ \mathcal{B}(D^{*+} \rightarrow D^+\gamma) &= (1.1_{-0.7}^{+2.1})\%\end{aligned}$$

CLEO has redone ¹⁰ the measurement of $\mathcal{B}(D^{*+} \rightarrow D^+\gamma)$ using ~ 5 times the amount of data as was used in the 1992 measurement. Again

the $D^+ \rightarrow K^- \pi^+ \pi^+$ decay mode is used. The most pernicious background is from $D_s^{*+} \rightarrow D_s^+ \gamma$ decays (the branching fraction is near 100%) where the D_s^+ decays to $K^- K^+ \pi^+$ ($\mathcal{B} = 4.6 \pm 1.2\%$) and the K^+ is misidentified as a π^+ . Recall that $M(D_s^{*+}) - M(D_s^+) = 143.97 \pm 0.41$ MeV while $M(D^{*+}) - M(D^+) = 140.64 \pm 0.09$ MeV so the two signals are not separated on the mass difference plot. These D_s^+ decays are explicitly vetoed in the new analysis by reconstructing a combination as $K^- K^+ \pi^+$ and only keeping combinations with $m(K^- K^+ \pi^+) > m(D_s^+)$. The signal is extracted from the plot of the mass difference, $M(K\pi\pi\gamma) - M(K\pi\pi) - (M_{D^{*+}} - M_{D^+})$, shown in Figure 4.

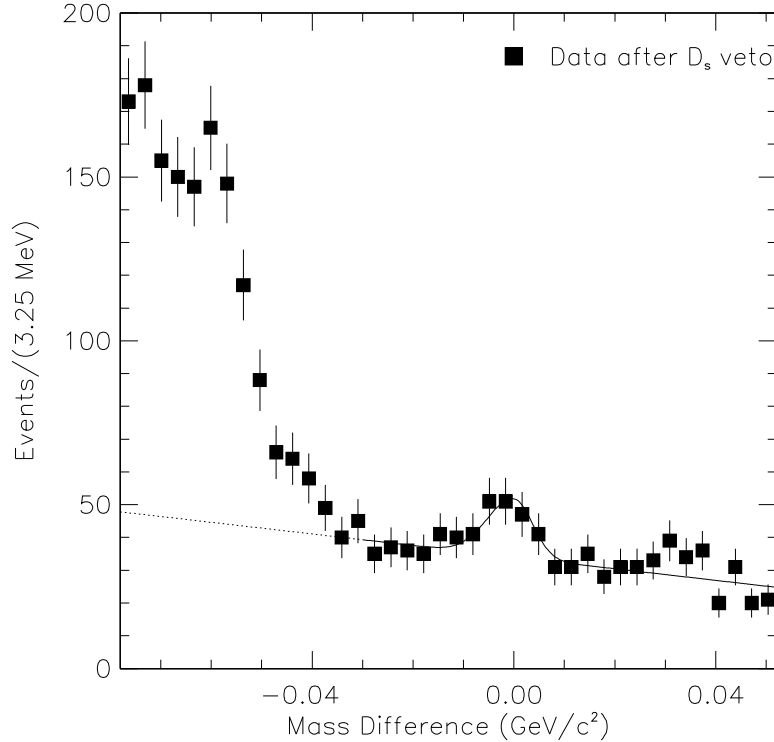


Figure 4: The mass difference $[M(K\pi\pi\gamma) - M(K\pi\pi) - (M_{D^{*+}} - M_{D^+})]$ for the CLEO data after the D_s^+ veto has been applied. The large peak on the left side of the plot is due to $D^{*+} \rightarrow D^+ \pi^0$ where one of the photons is lost. This process has been studied and found not to contribute the signal peak.

The new result is

$$\mathcal{B}(D^{*+} \rightarrow D^+\gamma) = (1.4 \pm 0.5 \pm 0.6)\%$$

While the near cancellation of magnetic moments suppresses the $D^{*+} \rightarrow D^+\gamma$ decay, the larger strange quark mass makes this effect even more pronounced in the $D_s^{*+} \rightarrow D_s^+\gamma$ case. Recall that there is no OZI-favored strong decay channel open to the D_s^{*+} and so, because of this strong suppression of the dominant decay, other suppressed decays may be non-negligible relative to $D_s^+\gamma$. In 1994, Cho and Wise¹² predicted that the isospin violating decay channel $D_s^{*+} \rightarrow D_s^+\pi^0$ could occur with a rate that is 1% to 10% of the $D_s^+\gamma$ rate. Further, using Chiral Perturbation Theory they predicted that the $D^{*+} \rightarrow D^+\gamma$ decay rate is related $D_s^{*+} \rightarrow D_s^+\pi^0$ decay rate. In 1995 CLEO observed this isospin violating decay mode and measured $\mathcal{B}(D_s^{*+} \rightarrow D_s^+\pi^0) = 0.058_{-0.016}^{+0.018} \pm 0.020$. The Cho and Wise theoretical calculation and the CLEO measurements are given in Figure 5.

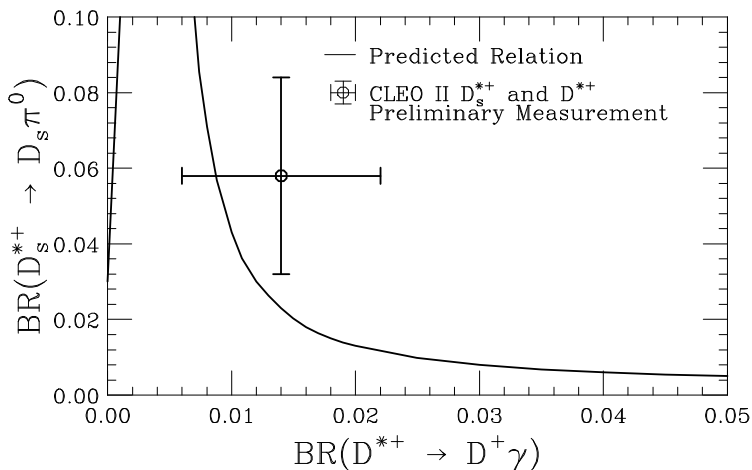


Figure 5: The relation predicted between the branching fractions for $D_s^{*+} \rightarrow D_s^+\pi^0$ and $D^{*+} \rightarrow D^+\gamma$ along with the CLEO measurements.

4 Charmed Baryon Spectroscopy – Filling up the Particle Data Booklet

There is a rich spectroscopy of charmed baryons, as seen in Table 1. All of the $J^P = \frac{1}{2}^+$ charmed baryons have been observed other than the Ξ'_c . The

$\Xi'_c \rightarrow \Xi_c \gamma$ decay mode should be a good one for CLEO to look into. Over the past year CLEO has observed^{13,14} the Ξ_c^{*0} and Ξ_c^{*+} having narrow widths, < 5.5 MeV and < 3.1 MeV, respectively, and mass differences of:

$$\begin{aligned} M(\Xi_c^+ \pi^-) - M(\Xi_c^+) &= 178.2 \pm 0.5 \pm 1.0 \text{ MeV} \\ M(\Xi_c^0 \pi^+) - M(\Xi_c^0) &= 174.3 \pm 0.5 \pm 1.0 \text{ MeV} \\ M(\Xi_c^{*0}) - M(\Xi_c^{*+}) &= -1.3 \pm 2.6 \text{ MeV} \end{aligned}$$

Quark Content Isospin and Spin of the (diquark)	$J^P = \frac{1}{2}^+$	$J^P = \frac{3}{2}^+$
$c(ud)$ $I = 0, S = 0$	Λ_c^+	
$c(uu, ud, dd)$ $I = 1, S = 1$	$\Sigma_c^{++}, \Sigma_c^+, \Sigma_c^0$	$\Sigma_c^{*++}, \Sigma_c^{*+}, \Sigma_c^{*0}$
$c(su, sd)$ $I = 1/2, S = 0$	Ξ_c^+, Ξ_c^0	
$c(su, sd)$ $I = 1/2, S = 1$	Ξ_c^{*+}, Ξ_c^{*0}	Ξ_c^{*+}, Ξ_c^{*0}
$c(ss)$ $I = 0, S = 0$	Ω_c^0	Ω_c^{*0}

Table 1: The S -wave charmed baryons.

So far the only evidence for the $J^P = \frac{3}{2}^+ \Sigma_c^*$ has been a cluster of 6 events in the $\Lambda_c^+ \pi^+$ channel observed in a heavy-liquid bubble chamber experiment.¹⁵ Now CLEO has evidence¹⁶ for both the Σ_c^{*++} and Σ_c^0 decaying to $\Lambda_c^+ \pi^+$ and $\Lambda_c^+ \pi^-$, respectively. Thirteen Λ_c^+ decay modes were utilized, with final states including a Σ^0 and Ξ^0 . This is made possible by the capability of CLEO to detect decay chains involving photons. Recall that the Σ^0 decays to $\Lambda \gamma$ essentially 100% of the time while $\Sigma^+ \rightarrow p \pi^0$ has a branching fraction of $\sim 50\%$ and $\mathcal{B}(\Xi^0 \rightarrow \Lambda \pi^0) \sim 100\%$.

The mass difference plots are shown in Figure 6. There are clear peaks around $\Delta M = 167$ MeV due to Σ_c decays and there is a broad enhancement around $\Delta M = 204$ MeV due to $\Lambda_c^{*+}(2630) \rightarrow \Lambda_c^+ \pi^+ \pi^-$ decays. These are taken into account in the fit to the mass difference plot. The results are given in Table 2. Both the mass difference and the width fall nicely within the theoretical expectations.¹⁷

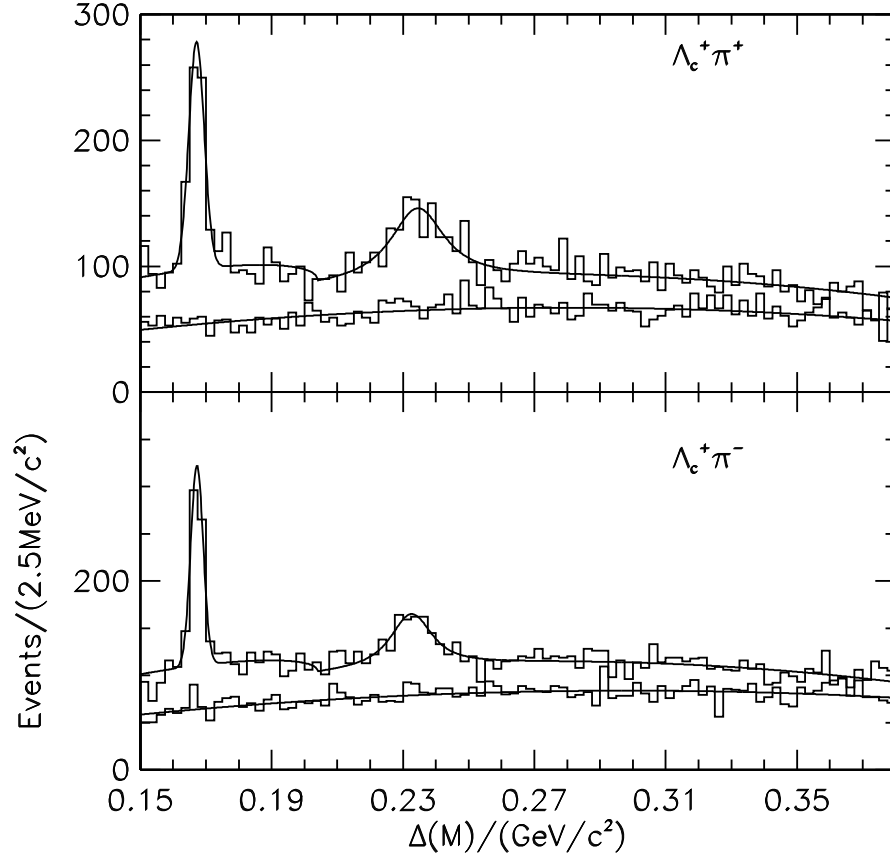


Figure 6: The $\Delta M \equiv m(\Lambda_c^+ \pi) - m(\Lambda_c)$ spectra from CLEO for (a) $\Lambda_c^+ \pi^+$, and (b) $\Lambda_c^+ \pi^-$.

	# Events	$M(\Lambda_c^+ \pi) - M(\Lambda_c^+) \text{ (MeV)}$	Width (MeV)
$\Lambda_c^+ \pi^+$	$677_{-93}^{+101} \pm 120$	$234.5 \pm 1.1 \pm 1.0$	$17.9_{-3.2}^{+3.8} \pm 4.0$
$\Lambda_c^+ \pi^-$	$504_{-83}^{+93} \pm 120$	$232.6 \pm 1.0 \pm 1.0$	$13.0_{-3.0}^{+3.7} \pm 4.0$

Table 2: The CLEO Σ_c^* results.

5 Weak Decays of Charmed Mesons

It is clear from the range of lifetimes given in Table 3 that there is much more to the dynamics of charmed hadron decay than is characterized just by the decay of the charm quark itself.

Charmed Hadron	Quark Content	Lifetime (ps)
D^+	$c\bar{d}$	1.057 ± 0.015
D^0	$c\bar{u}$	0.415 ± 0.004
D_s^+	$c\bar{s}$	0.467 ± 0.017
Λ_c^+	cud	0.206 ± 0.012
Ξ_c^+	csu	$0.35^{+0.07}_{-0.04}$
Ξ_c^0	csd	$0.098^{+0.023}_{-0.015}$
Ω_c^0	css	0.064 ± 0.020

Table 3: Summary of charmed hadron lifetimes (from PDG96).

Recall that for mesons $\hbar/\tau = \Gamma = \Gamma_{leptonic} + \Gamma_{semileptonic} + \Gamma_{nonleptonic}$. Each of the three processes in the charm sector uncovers a different aspect of QCD. Meson decay constants can be measured using purely leptonic decays while, because V_{cs} and V_{cd} are known precisely from the unitarity of the CKM Matrix, hadronic form factors can be extracted from semileptonic charm meson decay. This knowledge can then be used in the messy situation of nonleptonic charmed meson decays to gain information regarding final state interactions between the decay products. Various aspects of our understanding of the three contributions to the charmed meson total decay width will be discussed in the next three sections.

6 Leptonic Decays – Decay Constants, $D_s^+ \rightarrow \mu^+ \nu_\mu$, and Lattice QCD

Decay constants are a measure of the nonperturbative physics associated with quarks binding into mesons and are a source of great activity for those doing Lattice Gauge, QCD Sum Rules, and Quark Model calculations. Decay constants are important because they are often the largest source of uncertainty in extracting parameters of the Standard Model from measurements. For example, in $B^0 - \bar{B}^0$ mixing, the mixing parameter is given by:

$$x_d = \Delta M/\Gamma \propto V_{tb}^2 V_{td}^2 f_B^2 B_B m_t^2 F(m_t/m_W)^2$$

where F is a slowly varying function of m_t/m_W . With the present precision on m_t , the largest source of uncertainty in the extraction of V_{td} from measurements of x_d is the product of f_B , the B decay constant, and $\sqrt{B_B}$, where B_B is a parameter describing the degree to which the box diagrams dominate mixing. As another example, a calculation of the expected rate for the decay $B \rightarrow D^{*+}D^{*-}$, which is a mode with similar “ \mathcal{CP} reach” to the famous ψK final state¹⁸, requires knowledge of the D meson decay constant, f_D .

To see why there have been measurements of the D_s^+ decay constant, f_{D_s} , and not of f_D or f_B , consider the decay rate for the weak annihilation of a $Q\bar{q}$ pseudoscalar meson, M , into $\ell\nu$.

$$\Gamma(M^+ \rightarrow \ell^+\nu) = \frac{1}{8\pi} G_F^2 f_M^2 m_\ell^2 M_M \left(1 - \frac{m_\ell^2}{M_M^2}\right)^2 |V_{Qq}|^2$$

where M_M and m_ℓ are the masses of the meson and lepton, respectively, f_M is the pseudoscalar decay constant, and V_{Qq} is the relevant CKM matrix element. Helicity suppression is evident in the factor of m_ℓ^2 . The B^+ annihilation rates are predicted to be small (with a branching fraction of $\sim 10^{-5}$ for the least helicity suppressed channel $B^+ \rightarrow \tau^+\nu$) because the relevant CKM matrix element is V_{ub} . The charm annihilation rates are not small but the D_s^+ rates are Cabibbo favored over the D^+ (i.e., by roughly $|V_{cs}/V_{cd}|^2$) making the D_s^+ leptonic decay the most experimentally accessible.

CLEO published¹⁹ a measurement of $\Gamma(D_s^+ \rightarrow \mu^+\nu)/\Gamma(D_s^+ \rightarrow \phi\pi^+)$ in 1994 and updated²⁰ the measurement in 1995 using almost 50% more data and much improved measurements of the probability that a hadron is misidentified as a lepton (i.e., the lepton fake rates). The basic technique involved using the $D_s^{*+} \rightarrow D_s^+\gamma$ decay chain and the missing momentum and energy in an event to calculate the neutrino’s momentum. A key point to this analysis is that the $\mu^+\nu_\mu$ channel dominates over the $e^+\nu_e$ channel because of helicity suppression, but the backgrounds are essentially independent of lepton flavor. Hence, the analysis is performed for both electrons and muons, and whatever remains in the electron analysis is directly subtracted (taking into account the different lepton identification efficiencies) from the $\mu\nu$ sample.

A new measurement of $\mathcal{B}(D_s^+ \rightarrow \mu^+\nu_\mu)$ has been published²¹ by Fermilab experiment E653. They find the charm decay vertices in the emulsion and then tag the charge of the charmed hadron by the number of tracks associated with the vertex. In events where a muon is one of the decay products, the important variable is the transverse momentum $P_{T\mu}$ of the muon relative to the parent particle for vertices containing just the muon (one-prong “kinks”). The $P_{T\mu}$ distributions for “kinks” and neutral, two-prong vertices are given in Figures 7a) and 7b), respectively. The $D_s^+ \rightarrow \mu^+\nu_\mu$ signal appears as an

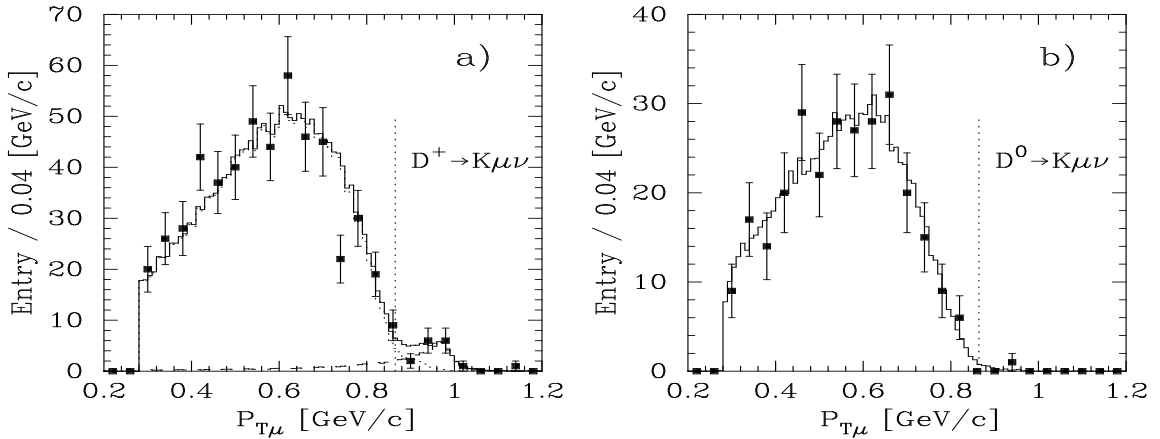


Figure 7: The $P_{T\mu}$ distributions from E653 for one-prong a) and two-prong b) muonic decay vertices.

excess number of events in the one-prong $P_{T\mu}$ distribution above the threshold for $D^+ \rightarrow \bar{K}^0 \mu^+ \nu_\mu$. There is a clear such excess in Figure 7a) whereas no excess is evident in the distribution for the neutral, two-prong vertices. The $D_s^+ \rightarrow \mu^+ \nu_\mu$ yield from a fit to this distribution is $23.2 \pm 6.0_{-0.9}^{+1.0}$ events. The number of background events from the Cabibbo suppressed $D^+ \rightarrow \mu^+ \nu_\mu$ channel and from $D_s^+ \rightarrow \tau^+ \nu_\tau$, $\tau^+ \rightarrow \mu^+ \nu_\mu \bar{\nu}_\tau$ are estimated to be 4.5 and 0.28, respectively. The final result is:

$$\frac{\mathcal{B}(D_s^+ \rightarrow \mu^+ \nu_\mu)}{\mathcal{B}(D_s^+ \rightarrow \phi \mu^+ \nu_\mu)} = 0.16 \pm 0.06 \pm 0.03$$

Renormalizing all results to the new value for $\mathcal{B}(D_s^+ \rightarrow \phi \pi^+)$ gives²² a world average branching fraction of $\mathcal{B}(D_s^+ \rightarrow \mu^+ \nu_\mu) = (4.6 \pm 0.8 \pm 1.2) \times 10^{-3}$. This translates into $f_{D_s} = (241 \pm 21 \pm 30)$ MeV where the systematic error is dominated by the uncertainty on $\mathcal{B}(D_s^+ \rightarrow \phi \pi^+)$. While there are a number of predictions for f_{D_s} using potential models and QCD sum rules, it is Lattice QCD which yields the least model dependent predictions. That is, in Lattice QCD the uncertainties due to the different assumptions can be systematically probed and estimated. It's rather interesting that Lattice QCD predictions appear much like experimental results with accompanying statistical and systematic errors ... and large authors lists! The world average result²³ from

Lattice QCD is $f_{D_s} = (235 \pm 15)$ MeV where the statistical and systematic errors have been combined in quadrature. We will soon reach the state where the uncertainty in $\mathcal{B}(D_s^+ \rightarrow \phi\pi^+)$ will be the dominant obstacle to a significant comparison of Lattice QCD with the experimental measurements of f_{D_s} .

7 Semileptonic Decays – More Results on Cabibbo Suppressed Decays

When both the initial and final state mesons in a semileptonic decay are pseudoscalars, the differential decay rate takes the particularly simple form:

$$\frac{d\Gamma}{dq^2} = \frac{G_F^2 |V_{Qq}|^2 P^3}{24\pi^3} \{ f_+(q^2) + m_l^2 f_-(q^2) \}$$

where P is the momentum of the final state meson in the rest frame of the decaying meson, q^2 is the invariant *mass*² of the virtual W , m_l is the mass of the lepton, and f_+ and f_- are form factors. The f_+ form factor dominates because of the m_l factor. Since V_{cs} and V_{cd} are known to good precision from unitarity of the CKM matrix,⁵ $f_+(q^2)$ can be measured directly. In particular, one would like to measure $f_+(q^2)$ in Cabibbo suppressed, heavy-to-light $c \rightarrow d$ transitions. This knowledge could then be used to test models of heavy-to-light transitions leading to smaller model uncertainties on the values for V_{ub} extracted from analyses of $b \rightarrow u\ell\nu$ decays.

The decay $D^0 \rightarrow \pi^-\ell^+\nu$ was observed²⁴ by Mark III (7 events) while CLEO reported²⁵ a signal of 87 ± 33 events. This is a difficult signal for CLEO since the pion is in a momentum range where their particle ID is not optimal for separating kaons from pions. This makes it difficult to suppress the Cabibbo favored $D^0 \rightarrow K^-\ell\nu$ decays.

The $D^0 \rightarrow h^-\ell^+\nu$ (where h is a meson) decay chain is well suited to a fixed target experiment where particle identification is somewhat easier and where silicon vertex detectors can be used to separate the secondary decay products from those coming from the primary vertex. E687 have published²⁶ results for $D^0 \rightarrow \pi^-\ell^+\nu$ and $D^0 \rightarrow K^-\ell^+\nu$ decays for both electrons and muons. They use the $D^{*+} \rightarrow D^0\pi^+$ decay chain to further reduce combinatoric backgrounds. The secondary vertex containing the $h^-\ell^+$ pair satisfies a separation cut of $(l/\sigma_l) > 4$ and it is required to be isolated from all other tracks in the event. The electron and muon channels contain 45.4 ± 13.3 events and 45.6 ± 11.8 events, respectively.

Unfortunately no experiment yet has a sample large enough to allow for a measurement of the q^2 dependence of the form factor. The result for the ratio of form factors from E687 is $|f_+^\pi(0)/f_+^K(0)| = 1.00 \pm 0.11 \pm 0.02$ while the CLEO

value for this ratio was $1.01 \pm 0.20 \pm 0.07$. CLEO has also remeasured²⁷ $\mathcal{B}(D^+ \rightarrow \pi^0 \ell^+ \nu) / \mathcal{B}(D^+ \rightarrow \pi^0 \ell^+ \nu)$ and found $|f_+^\pi(0) / f_+^K(0)|^2 = 0.9 \pm 0.3 \pm 0.3$. The world average, assuming $|V_{cd} / V_{cs}|^2 = 0.051 \pm 0.01$, becomes $|f_+^\pi(0) / f_+^K(0)| = 0.99 \pm 0.08$. Theoretical predictions range from 0.7 to 1.4 for this ratio.

The exploration of Cabibbo suppressed semileptonic charm meson decays to vector final states has just begun with the report²⁸ from E687 of the first statistically significant signal for $D \rightarrow \rho \ell \nu$. Measurements involving vector final states and extraction of the q^2 dependence of the form factors should be the experimental goals for the near future.

8 Nonleptonic Decays – The Spectre of $D_s^+ \rightarrow \omega \pi^+$ and The Puzzle of $D_s^+ \rightarrow \eta' \rho^+$

There are a number of puzzles in hadronic D_s^+ decays although none are as intriguing at present as the $D_s^+ \rightarrow \eta' \rho^+$ branching fraction. The PDG96 values (consisting solely of the old CLEO results²⁹) along with the new³⁰ CLEO results for $D_s^+ \rightarrow \eta \rho^+$ and $D_s^+ \rightarrow \eta' \rho^+$ are given in Table 4. Besides

	CLEO-II (1992)	CLEO-II (ICHEP 1996)
$\frac{\Gamma(D_s^+ \rightarrow \eta \rho^+)}{\Gamma(D_s^+ \rightarrow \phi \pi^+)}$	$2.86 \pm 0.38_{-0.38}^{+0.36}$	$2.98 \pm 0.20 \pm 0.39$
$\frac{\Gamma(D_s^+ \rightarrow \eta' \rho^+)}{\Gamma(D_s^+ \rightarrow \phi \pi^+)}$	$3.44 \pm 0.62_{-0.46}^{+0.44}$	$2.78 \pm 0.28 \pm 0.30$

Table 4: Status of measurements of D_s^+ decays to $\eta \rho^+$ and $\eta' \rho^+$.

just an increase of statistics, the new CLEO number for $\mathcal{B}(D_s^+ \rightarrow \eta \rho^+)$ results from a full Dalitz analysis of the $\eta \pi^+ \pi^0$ final state. The four Dalitz plots used in the analysis are shown in Figure 8. The $\eta \pi^+ \pi^0$ Dalitz plots are:

- (a) for the D_s^+ signal region defined by $1.94 < m(\eta \pi^+ \pi^0) < 1.99$ GeV,
- (b) for the D_s^+ sideband region defined by $1.75 < m(\eta \pi^+ \pi^0) < 1.90$ GeV and $2.04 < m(\eta \pi^+ \pi^0) < 2.24$ GeV,
- (c) for pure $D_s^+ \rightarrow \eta \rho^+$ Monte Carlo signal,
- (d) for non-resonant $\eta \pi^+ \pi^0$ Monte Carlo generated according to phase space.

It is clear from Figure 8(a) that there is little non-resonant contribution. The value in Table 4 is the product of fitting the histogram of Figure 8(a) with a function containing the (b), (c), and (d) histograms.

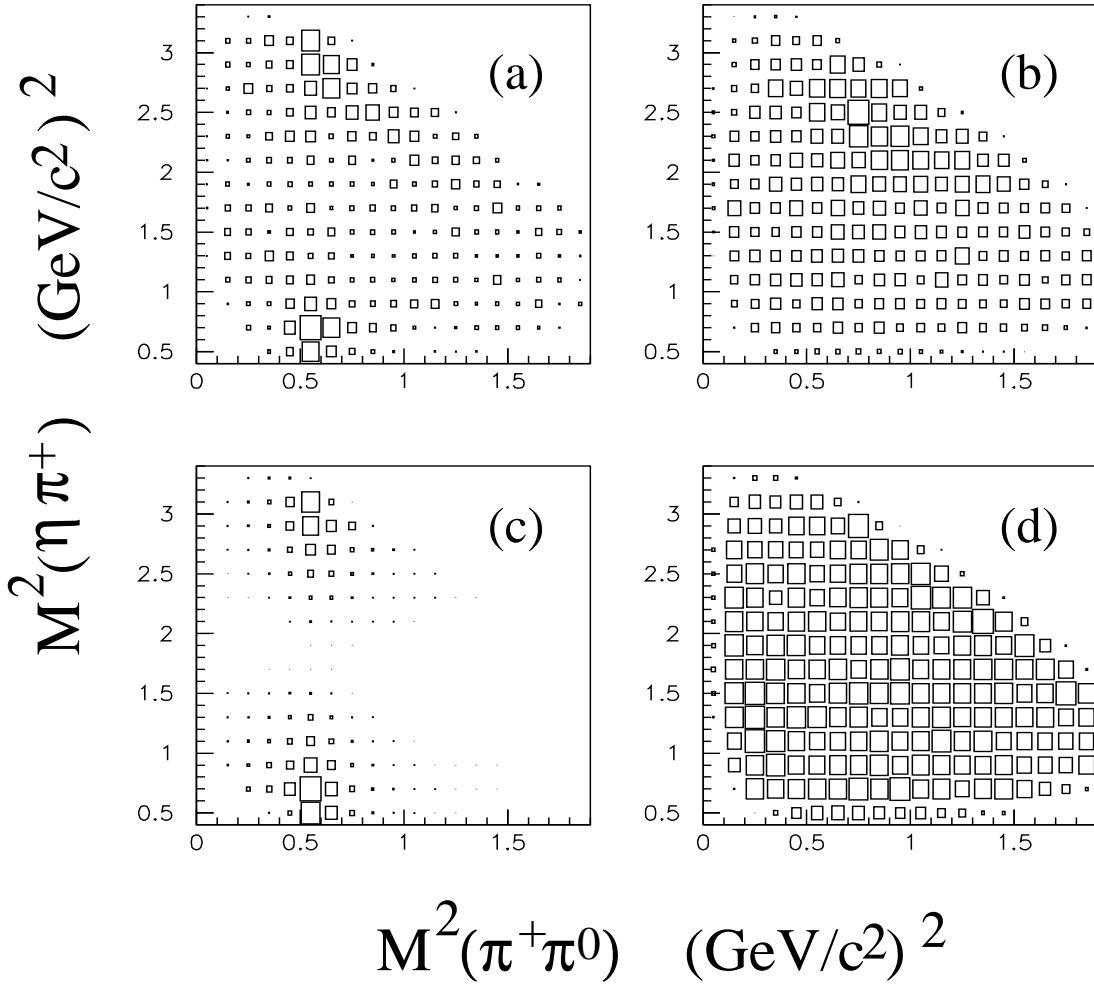


Figure 8: Dalitz plot of $D_s^+ \rightarrow \eta\pi^+\pi^0$, $\eta \rightarrow \gamma\gamma$ for: (a) Data D_s^+ mass signal region; (b) Data D_s^+ mass sidebands; (c) MC signal; (d) MC simulation of non-resonant $\eta\pi^+\pi^0$ (generated according to phase space).

These new CLEO results confirm that $\mathcal{B}(D_s^+ \rightarrow \eta' \rho^+) \approx \mathcal{B}(D_s^+ \rightarrow \eta \rho^+)$. This is somewhat surprising since the limited phase space suppresses the η' mode by a factor of 3 to 4 relative to $\eta \rho^+$. Two groups of theorists – Hinchliffe and Kaeding³¹, and Buccella, Lusignoli, and Pugliese³² – have found a good description of nonleptonic charmed meson decays using the factorization ansatz³³ and including annihilation, final state interactions, etc. Neither of these papers can account for the large value for $\mathcal{B}(D_s^+ \rightarrow \eta' \rho^+)$. The ratio of $\mathcal{B}(D_s^+ \rightarrow \eta' \rho^+)$ to $\mathcal{B}(D_s^+ \rightarrow \phi \pi^+)$ is predicted in the Hinchliffe and Buccella papers to be 0.43 and 0.59, respectively. Just to emphasize the seriousness of the problem that this mode introduces, here is what is said about this mode in the Hinchliffe paper where they have fit their model to some 53 different branching fractions;

“The total χ^2 (of the fit) was found to be 30.9 for seven degrees of freedom, indicating that the overall fit was poor. However, more than half of the χ^2 arose from only one mode. The mode in question is $D_s^+ \rightarrow \eta' \rho^+$. The experimental value for $\mathcal{B}(D_s^+ \rightarrow \eta' \rho^+)$ cannot be accommodated in our scheme..... We decided to reject the experimental value for the branching fraction of $D_s^+ \rightarrow \eta' \rho^+$. The result is a better fit. The total χ^2 is now 11.6 for six degrees of freedom.”

The other result which does not fit easily into our understanding of hadronic D_s^+ decays is the recent measurement³⁴ from CLEO:

$$\frac{\mathcal{B}(D_s^+ \rightarrow \omega \pi^+)}{\mathcal{B}(D_s^+ \rightarrow \eta \pi^+)} = 0.16 \pm 0.04 \pm 0.03$$

As we will see, this final state can only be produced in a rather unconventional way without final state interactions.

First consider nonleptonic D_s^+ decays ignoring final state interactions. For convenience, the final state mesons and their relevant characteristics are listed in Table 5. The η and η' quark contents given in the Table are, of course, just those of the $SU(3)$ octet and singlet states – the η_8 and η_1 . A non-zero $\eta - \eta'$ mixing angle does not have an appreciable effect on what follows.

The spectator decay diagram, shown in Figure 9, can lead to a final state consisting of any combination of (ϕ, η, η', f_0) and (π^+, ρ^+) . The D_s^+ is also massive enough to decay to ηa_1 and $\eta' a_1$.

The next first order diagram is the helicity-suppressed annihilation diagram shown in Figure 10. The question of the strength (or the very existence) of this diagram came up about 8 years ago when E691 produced³⁵ its limits on $\omega \pi^+$ and $\rho^0 \pi^+$. The definitive argument on what final states are allowed via

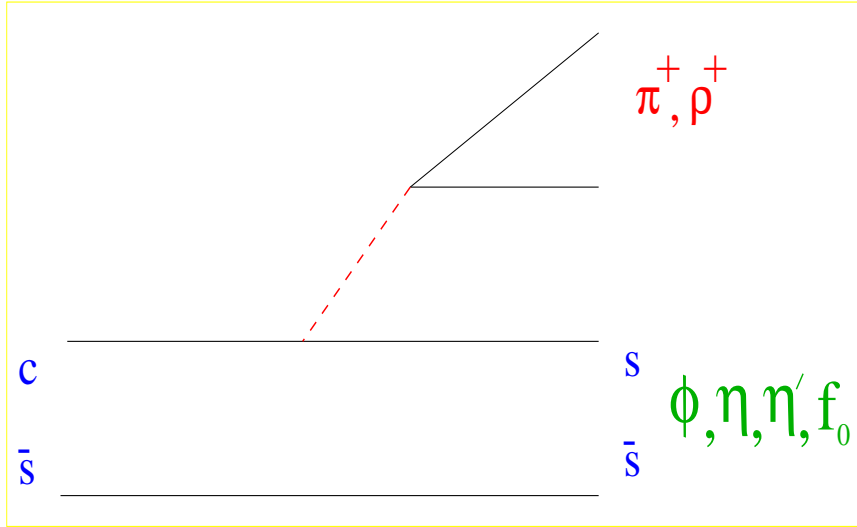


Figure 9: The D_s^+ spectator decay diagram.

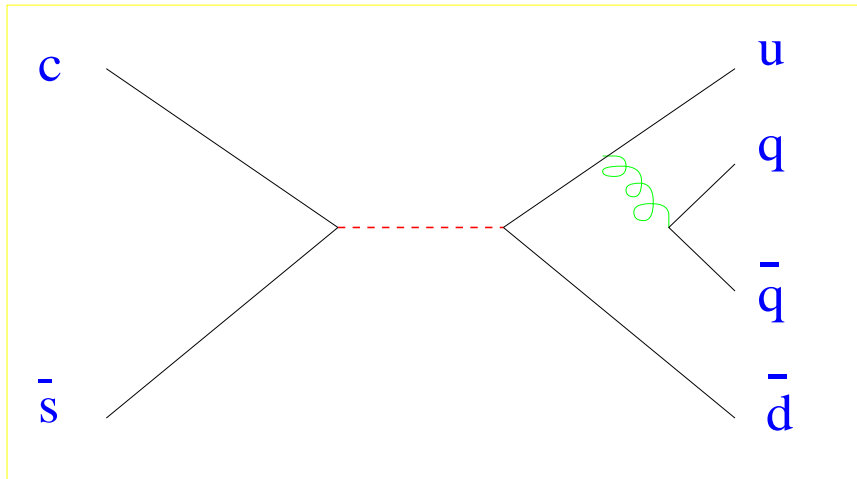


Figure 10: The D_s^+ annihilation decay diagram (\mathcal{A}).

Meson	Mass (MeV)	J^P	I	G -parity	quark content
π^+	139.7	0^-	1	-1	$u\bar{d}$
π^0	134.98	0^-	1	-1	$u\bar{u} - d\bar{d}$
ρ^+	768.5	1^-	1	+1	$u\bar{d}$
ρ^0	768.5	1^-	1	+1	$u\bar{u} - d\bar{d}$
ω	781.94	1^-	0	-1	$u\bar{u} + d\bar{d}$
ϕ	1019.41	1^-	0	-1	$s\bar{s}$
η	547.45	0^-	0	+1	$u\bar{u} + d\bar{d} - 2s\bar{s}$
η'	957.77	0^-	0	+1	$u\bar{u} + d\bar{d} + s\bar{s}$
f_0	980	0^+	0	+1	$s\bar{s}$ (?)

Table 5: Characteristics of the final state mesons considered in this note.

annihilation was made by Harry Lipkin,³⁶ using two different techniques. One version of the argument goes as follows. When you annihilate a D_s^+ into a $u\bar{d}$ state, some quantum numbers of the final state are known: $J = 0$, $I = 1$ (the $u\bar{d}$ has $I_3 = 1$, therefore $I = 1$) and $G = -1$. These quantum numbers will not change in the hadronization process, which is a strong interaction. The allowed final states are: $\rho^0\pi^+$, $\rho^+\pi^0$, $\eta\pi^+$, $\eta'\pi^+$, $\omega\rho^+$, and $f_0\pi^+$. The decay channels forbidden by G -parity conservation are: $\omega\pi^+$, $\pi^0\pi^+$, $f_0\rho^+$, $\eta\rho^+$, $\eta'\rho^+$, and $\rho^0\rho^+$.

Neither of these diagrams result in $D_s^+ \rightarrow \omega\pi^+$ or ^b favor $D_s^+ \rightarrow \eta'\rho^+$. Gluon emission from the final state quark lines does not break the G -parity argument given above but gluon emission from the initial quark lines is allowed and also helps to mitigate the helicity suppression. At least two gluons must be emitted since the W is colorless. Two diagrams illustrative of the case where two gluons are emitted are shown in Figures 11 and 12. Figure 12 and the three gluon emission diagram of Figure 13 are sometimes referred to as the “hairpin” diagrams and can lead to enhanced $D_s^+ \rightarrow \eta'\rho^+$ and $D_s^+ \rightarrow \omega\pi^+$ rates. Since coupling of the gluons to the quarks is independent of flavor, the final state is an equal mixture of $u\bar{u}$, $d\bar{d}$, and $s\bar{s}$, i.e., the final $q\bar{q}$ final state is an $SU(3)$ flavor singlet, with presumably some suppression of the $s\bar{s}$ component depending on the available energy. The two-gluon final state is \mathcal{C} even giving an η' (and f_0 ??). The \mathcal{C} odd, $SU(3)$ singlet vector mesons, the ω and ϕ , are produced by three gluons, presumably with relative strengths of 2:1 based on

^bSince the the $SU(3)$ singlet vector mesons, the ω and ϕ are not completely $u\bar{u} + d\bar{d}$ and $s\bar{s}$, respectively, the spectator diagram does lead to a small $D_s^+ \rightarrow \omega\pi^+$ branching fraction. An octet-singlet mixing angle⁵ of 39° gives a naive estimate of $\mathcal{B}(D_s^+ \rightarrow \omega\pi^+) \sim 0.004 \times \mathcal{B}(D_s^+ \rightarrow \phi\pi^+)$, well below the observed rate.

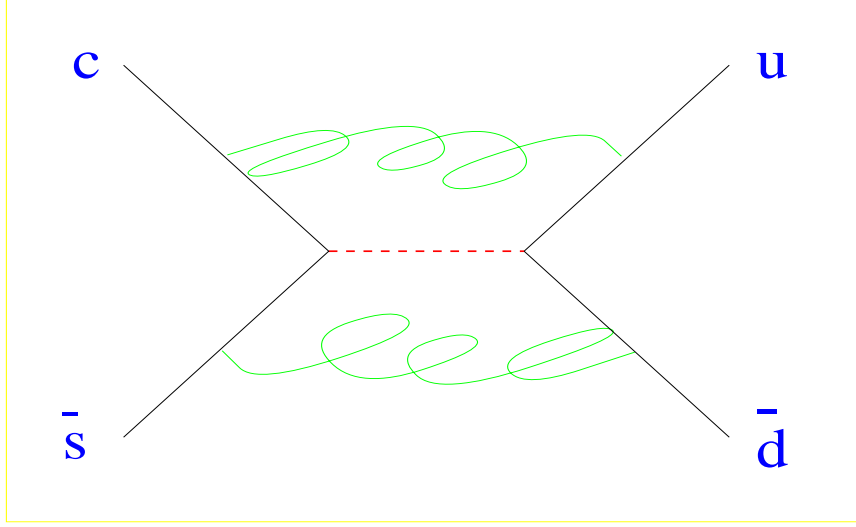


Figure 11: The D_s^+ annihilation decay diagram (\mathcal{A}_{G2}) with two gluon emission from the initial quark lines.

their quark content. This diagram does not lead to a π^0 , ρ^0 , or η in the final state.^c Charmonium decays can give some guide as to the relative strengths of the two- and three-gluon decays. The $\eta_c(2980)$ and the $\psi(3097)$ have widths of 10 MeV and 88 KeV, respectively, so there is a factor 100 suppression due to the extra gluon. This is at the high energy scale where α_s is small. One could guess there might be an extra factor of 10 suppression (3 in the amplitude) for three gluons compared to two gluons at the mass scale of the $\omega/\eta/\phi$.

The following nomenclature will be used for the different decay amplitudes:

\mathcal{S} – external W (spectator),

\mathcal{A} – pure annihilation

\mathcal{A}_{G2} – 2 gluons + annihilation,

\mathcal{H}_{G2} – 2 gluon “hairpin”,

\mathcal{H}_{G3} – 3 gluon “hairpin”,

^cThis is not absolutely correct in the presence of η - η' mixing, although the η contribution would be $\tan^2 \theta_{mix}$ (or around 3% for $\theta_{mix} = -10.1^\circ$) that of η' .

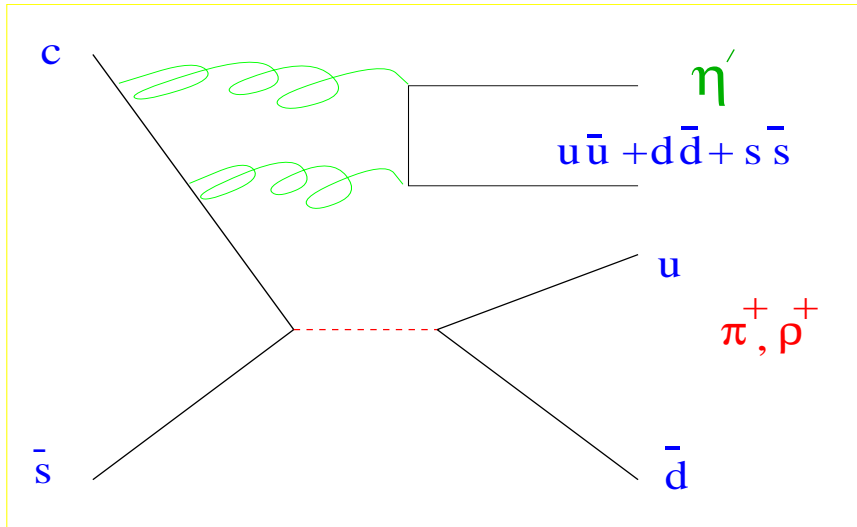


Figure 12: The two gluon "hairpin" diagram (\mathcal{H}_{G2}).

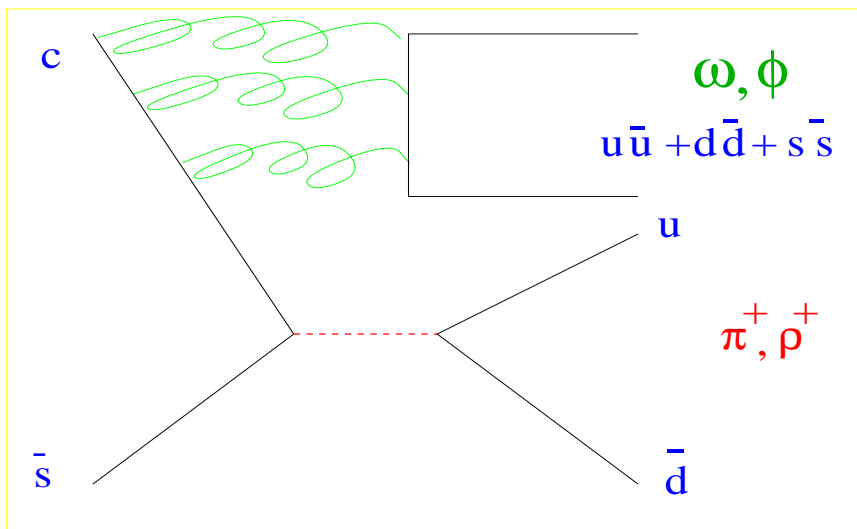


Figure 13: The three gluon "hairpin" diagram (\mathcal{H}_{G3}).

Presumably \mathcal{S} is much larger than any of the other contributions.

Ignoring phase space factors, decay constants, etc., naive estimates for the decay amplitudes for the various decay channels are then:

$$\begin{aligned}
\mathcal{A}(D_s^+ \rightarrow \phi\pi^+) &\propto \mathcal{S} \pm \sqrt{\frac{1}{3}}\mathcal{H}_{\mathcal{G}3} \\
\mathcal{A}(D_s^+ \rightarrow \phi\rho^+) &\propto \mathcal{S} \pm \sqrt{\frac{1}{3}}\mathcal{H}_{\mathcal{G}3} \\
\mathcal{A}(D_s^+ \rightarrow \eta\pi^+) &\propto \sqrt{\frac{2}{3}}\mathcal{S} \pm \sqrt{\frac{1}{3}}\mathcal{A} \pm \sqrt{\frac{1}{3}}\mathcal{A}_{\mathcal{G}2} \\
\mathcal{A}(D_s^+ \rightarrow \eta'\pi^+) &\propto \sqrt{\frac{1}{3}}\mathcal{S} \pm \sqrt{\frac{2}{3}}\mathcal{A} \pm \sqrt{\frac{2}{3}}\mathcal{A}_{\mathcal{G}2} \pm \mathcal{H}_{\mathcal{G}2} \\
\mathcal{A}(D_s^+ \rightarrow \eta\rho^+) &\propto \sqrt{\frac{2}{3}}\mathcal{S} \pm \sqrt{\frac{1}{3}}\mathcal{A}_{\mathcal{G}2} \\
\mathcal{A}(D_s^+ \rightarrow \eta'\rho^+) &\propto \sqrt{\frac{1}{3}}\mathcal{S} \pm \sqrt{\frac{2}{3}}\mathcal{A}_{\mathcal{G}2} \pm \mathcal{H}_{\mathcal{G}2} \\
\mathcal{A}(D_s^+ \rightarrow \omega\pi^+) &\propto \sqrt{\frac{2}{3}}\mathcal{H}_{\mathcal{G}3} \pm \mathcal{A}_{\mathcal{G}2} \\
\mathcal{A}(D_s^+ \rightarrow \omega\rho^+) &\propto \mathcal{A} + \sqrt{\frac{2}{3}}\mathcal{H}_{\mathcal{G}3} \pm \mathcal{A}_{\mathcal{G}2} \\
\mathcal{A}(D_s^+ \rightarrow \rho^0\pi^+) &\propto \mathcal{A} \pm \mathcal{A}_{\mathcal{G}2} \\
\mathcal{A}(D_s^+ \rightarrow \rho^+\pi^0) &\propto \mathcal{A} \pm \mathcal{A}_{\mathcal{G}2}
\end{aligned}$$

where the coefficients are quark content factors. The relative phase (sign) of the different contributions is not known *a priori* and has been left free. Recall from the previous argument that we might expect $\mathcal{H}_{\mathcal{G}2} \approx 3\mathcal{H}_{\mathcal{G}3}$. As a final note, the doubly-Cabibbo suppressed decay, $c\bar{s} \rightarrow d\bar{s}W^+ \rightarrow d\bar{s}u\bar{s}$, leads to two \bar{s} quarks in the final state and so does not contribute here.

This naive analysis uncovers several interesting facets of these decays. The $D_s^+ \rightarrow \omega\pi^+$ mode is only produced through the “exotic” diagrams involving the emission of some number of gluons followed by annihilation. It is not clear whether the G -parity arguments used to restrict the final states in pure annihilation are applicable to $\mathcal{A}_{\mathcal{G}2}$ as well. If they were, then the $D_s^+ \rightarrow \omega\pi^+$ decay mode would represent the “smoking gun” for the 3-gluon plus annihilation decay mechanism except. As usual, final state interactions will be seen to complicate such an interpretation. If the diagram of Figure 12 does at least contribute somewhat, then modes involving the $\mathcal{H}_{\mathcal{G}2}$ amplitude would be correspondingly enhanced or suppressed depending on the relative phase of

the two contributions. For example,

$$\frac{\Gamma(D_s^+ \rightarrow \eta' \rho^+)}{\Gamma(D_s^+ \rightarrow \eta \rho^+)} \propto \frac{(\mathcal{S} \pm \mathcal{H}_{G2})^2}{\mathcal{S}^2}$$

The experimental data could be explained if the relative sign were positive leading to constructive interference. However, \mathcal{H}_{G2} would have to be very large compared to \mathcal{S} which only seems possible if the η' were to have an anomalously large gluonic component. These relations, however, are strongly affected by final state interactions, as discussed next.

All quantum numbers are conserved in strong interactions between the final state mesons (so-called final state interactions or FSI). It seems reasonable that significant FSI can occur if the intermediate mesons are in a configuration with the quantum numbers of some resonance.³⁷ This leads to the argument, for example, that you cannot get $D_s^+ \rightarrow \omega \pi^+$ through FSI since the ω and π^+ are in a $J^P = 0^-, I^G = 1^+$ state and there is no resonance with this combination of quantum numbers. The key word here is “significant” since non-resonant FSI may be very much reduced in amplitude relative to this “intermediate resonance” type of FSI but it may be significant relative to \mathcal{H}_{G2} . It is hard to know how to deal with this. Consider $D_s^+ \rightarrow \omega \pi^+$. The $D_s^+ \rightarrow \omega \pi^+$ branching fraction was predicted to be identically 0 in the original attempt by Buccella *et al.* at describing nonleptonic charmed meson decays.³⁸ This model included only “resonant” FSI and did not include the diagram of Figure 13. However, the more recent version of their model³² does contain “non-resonant” FSI, although the 3-gluon + annihilation amplitude \mathcal{H}_{G3} is still absent. The model contains 11 free parameters and they fit some 49 charmed meson branching fractions. From the results of the fit they predict:

$$\frac{\mathcal{B}(D_s^+ \rightarrow \omega \pi^+)}{\mathcal{B}(D_s^+ \rightarrow \eta \pi^+)} = 0.21$$

— essentially what is observed. So, as usual, FSI of some type just completely muddies the picture, at least with respect to modes with small widths from the “standard” decay mechanisms. That is, clearly even a small amount of rescattering from a large mode into a suppressed or disallowed mode will have a huge relative effect on the small mode and almost none on the large mode. The main point is that there is a model which predicts (not postdicts!) the $D_s^+ \rightarrow \omega \pi^+$ rate without resorting to “exotic” decay mechanisms like that of Figure 13.

What of $D_s^+ \rightarrow \eta' \rho^+$? The following is from the Buccella paper;

*Concerning the decay rates of D_s^+ and D^0 , the quality of the present fit is comparable to the fit in*³⁸ (i.e., the first attempt which did not

include “non-resonant” FSI). *In particular, for $D^0 \rightarrow \bar{K}^{*0}\eta$ and $D_s^+ \rightarrow \eta'\rho^+$ the results are still unsatisfactory (more than three standard deviations lower than the data points). Neither annihilation contributions, nor final state interactions were present for channels with positive G -parity and $I = 1$, like $\eta'\rho^+$, in ³⁸. In this fit the exotic rescattering affects these channels, giving for instance a nonzero branching ratio for the decay $D_s^+ \rightarrow \omega\pi^+$; however, it only slightly lowers (going in the wrong direction) the theoretical prediction for $\mathcal{B}(D_s^+ \rightarrow \eta'\rho^+)$.*

It is reasonably easy to see how this could happen. Consider what could rescatter into $\eta\rho^+$ and $\eta'\rho^+$. The “big” amplitudes are the external and internal W diagrams. Just as in the $\omega\pi^+$ case, the $\eta\rho^+$ and $\eta'\rho^+$ final states are in a $J^P = 0^-, I^G = 1^+$ configuration and so cannot rescatter through “significant” intermediate resonance FSI. Of course, $\phi\pi^+$ can scatter into $\eta(\eta')\rho^+$ through non-resonant FSI. However, since $\mathcal{B}(D_s^+ \rightarrow \eta'\rho^+)$ is so much larger than $\mathcal{B}(D_s^+ \rightarrow \phi\pi^+)$, this mechanism would naturally deplete $D_s^+ \rightarrow \eta'\rho^+$, as observed seen in the Buccella *et al.* paper. Also, there is the p^3 term in the rates which always disfavors $D_s^+ \rightarrow \eta'\rho^+$. Finally, it should be noted that a large value for $\mathcal{B}(D_s^+ \rightarrow \omega\pi^+)$ was predicted in the Buccella paper due to FSI even though they are still far off on the prediction for $\mathcal{B}(D_s^+ \rightarrow \eta'\rho^+)$. Hence, it appears that they would get an unacceptably large value for $\mathcal{B}(D_s^+ \rightarrow \omega\pi^+)$ if $\mathcal{B}(D_s^+ \rightarrow \eta'\rho^+)$ was five times larger, as indicated by the data. Further, the values for $\mathcal{B}(D_s^+ \rightarrow \rho^0\pi^+)$ and $\mathcal{B}(D_s^+ \rightarrow \rho^+\pi^0)$ in the Buccella model are already larger than experimental upper limits so this model should not, in any scenario, be considered the final word on the subject.

The internal W , color suppressed decay diagram (i.e., the \mathbf{a}_2 diagram in factorization language) is shown in Figure 14. The $\bar{K}^{(*)0}K^{(*)+}$ final state is a $J = 0, I = 1$ configuration, just as in annihilation, and so has $G = -1$. Hence, from G -parity, it is forbidden to rescatter into $\eta\rho^+$ and $\eta'\rho^+$ while $\eta\pi^+$ and $\eta'\pi^+$ are allowed.

The \mathcal{H}_{G2} mechanism would naively boost $D_s^+ \rightarrow \eta'X/D_s^+ \rightarrow \eta X$ for any particle X although FSI affect the $\eta(\eta')\rho^+$ final states differently than the $\eta(\eta')\pi^+$ final states. There is a paper by Ball and collaborators³⁹ in which a gluonic content to the η and η' is hypothesized based on various phenomenological considerations. It is written in this paper that:

Having a rather comprehensive view of the η and η' system and its connection with glue, we now address other promising channels for future investigations, to wit D_s decays. Here two processes compete to produce $\eta(\eta')X$ final states: The first one is the decay $c \rightarrow s$,

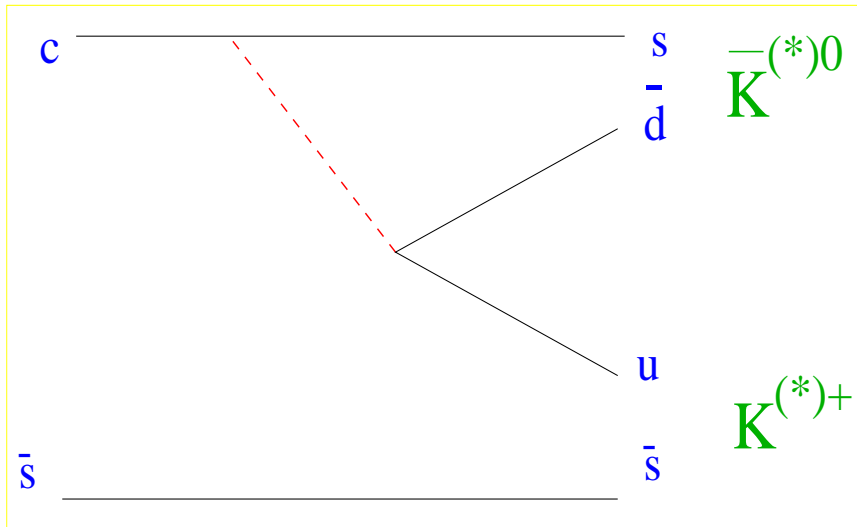


Figure 14: The internal W D_s^+ decay diagram.

leading to an $\bar{s}s$ pair, which hadronizes to η or η' , while the second one can be described as $c\bar{s}$ annihilation into W and two gluons. It is suppressed by the Zweig-rule, but may in the present case gain importance through the large $\langle 0|G\tilde{G}|\eta(\eta')\rangle$ matrix elements. We should thus expect both an enhancement of the $(\eta + \eta')X$ modes (unless interference is destructive) and a large η'/η ratio, once the rates are corrected for phase-space and final state interactions.

So there is at least some reason to believe that the diagram of Figure 12 may play a not insignificant role in D_s^+ decays.

As usual in nonleptonic charm decays, we are left in the position that the lack of a quantitative understanding of final state interactions precludes connecting the experimental data to any particular underlying physical decay mechanism. The $D_s^+ \rightarrow \omega\pi^+$ branching fraction can be explained by at least one model which includes final state interactions. The large value of $\mathcal{B}(D_s^+ \rightarrow \eta'\rho^+)$ is difficult to explain theoretically although one decay process – annihilation plus two gluons – does seem to feed preferentially into this mode and could be the explanation. It would be interesting to find other decay channels that need this mechanism and try to measure them.

9 Conclusions

The field of charm physics is at present being driven by experiment. And experimental charm physics will only get healthier in the near future with the high statistics charm experiments FOCUS and SELEX currently running at Fermilab, CLEO continuing to collect and analyze data, and still to be analyzed data from LEP, HERA, and BEPC. The turn of the century should see a high luminosity CESR feeding a CLEO detector with improved particle identification capabilities and a silicon vertex detector (CLEO-III) as well as the turn on of B Factories at KEK and SLAC. It would be nice to see the machinery of Lattice QCD turned towards solving some of the mysteries in charm decays, like the amplitudes and phases associated with final state interactions. Hopefully the nonperturbative regime of QCD can finally be conquered theoretically and all of this data can be used to prove or disprove the theory of the strong force.

Acknowledgments

I benefited greatly from conversations with many of my CLEO collaborators, in particular Vivek Jain, Rob Kutschke, Rollin Morrison, and Mike Witherell. I would also like to thank Harry Cheung (E687), Eugene Chudakov (WA89), Rob Gardner (E687), Milind Purohit (E791), and Mike Sokoloff (E791) for responding to my call for information on new results from their experiments.

References

1. When a particular state or reaction is referred to, the charge conjugate state or reaction is implicitly included unless stated otherwise.
2. see Jean Slaughter's contribution to these proceedings.
3. see Paul Karchin's contribution to these proceedings.
4. For example, BES Collaboration, J.Z. Bai *et al.*, "*Search for a Vector Glueball by a Scan of the J/ψ Resonance*", Phys. Rev. **D54**, 1221 (1996).
5. Particle Data Group, R.M. Barnett *et al.*, Review of Particle Physics, Phys. Rev. **D54**, 1 (1996).
6. Particle Data Group, L. Montanet *et al.*, Review of Particle Properties, Phys. Rev. **D50**, 1 (1994).
7. CLEO Collaboration, M. Artuso *et al.*, Phys. Lett. **B378**, 364 (1996).
8. Mark III Collaboration, J. Adler *et al.*, Phys. Lett **B208**, 152 (1988).
9. CLEO Collaboration, F. Butler *et al.*, Phys. Rev. Lett. **69**, 2041 (1992).

10. CLEO Collaboration, M. S. Alam *et al.*, CLEO-CONF 96-7, paper submitted to the 28th International Conference on High-energy Physics, Warsaw, Poland (1996). A postscript version can be found at <http://w4.lns.cornell.edu/public/CONF/1996/>.
11. R. Kutschke, “*Heavy Flavour Spectroscopy*”, Lectures presented at the NATO Advanced Study Institute on *Hadron Spectroscopy and the Confinement Problem*, London, 1995.
12. P. Cho and M. B. Wise, Phys. Rev. **D49**, 6228 (1994).
13. CLEO Collaboration, P. Avery *et al.*, Phys. Rev. Lett. 75, 4364 (1995).
14. CLEO Collaboration, L. Gibbons *et al.*, Phys. Rev. Lett. 77, 810 (1996).
15. V. Ammosov *et al.*, JETP Letters **58**, 247 (1993).
16. CLEO Collaboration, G. Brandenburg *et al.*, CLNS 96/1427 (1996), submitted to Phys. Rev. Lett. A postscript version can be obtained at <http://w4.lns.cornell.edu/public/CLNS/1996>
17. J. L. Rosner, “*Charmed Baryons with $J = 3/2$* ”, hep-ph/9508252.
18. The BaBar Technical Design Report, SLAC-R-95-457, (1995).
19. CLEO Collaboration, D. Acosta *et al.*, Phys. Rev. **D49**, 5690 (1994).
20. CLEO Collaboration, D. Gibaut *et al.*, CLEO-CONF 95-22 (EPS-0184), submitted to the European Physical Society Conference, Brussels, Belgium (1995). A postscript version can be obtained at <http://w4.lns.cornell.edu/public/CONF/1995>
21. Fermilab E653 Collaboration, K. Kodama *et al.*, Phys. Lett. **B382**, 299 (1996).
22. J. D. Richman, “*Progress in Understanding Heavy Flavor Decays*”, invited talk at 28th International Conference on High-energy Physics, Warsaw, Poland, (1996).
23. J. M. Flynn, “*Developments in Lattice QCD*”, hep-lat/9611016.
24. Mark III Collaboration, J. Adler *et al.*, Phys. Rev. Lett 62, 1821 (1989).
25. CLEO Collaboration, F. Butler *et al.*, Phys. Rev. **D52**, 2656 (1995).
26. E687 Collaboration, P. L. Frabetti *et al.*, Phys. Lett. **B382**, 312 (1996).
27. CLEO Collaboration, J. Bartelt *et al.*, “*Studies of the Cabibbo-suppressed decays $D^+ \rightarrow \pi^0 e^+ \nu_e$ and $D^+ \rightarrow \eta e^+ \nu_e$* ”, CLNS 97/1460, submitted to Phys. Lett. **B**. A postscript version can be obtained at <http://w4.lns.cornell.edu/public/CLNS/1997>
28. E687 Collaboration, P. L. Frabetti *et al.*, FERMILAB-Pub-96/388-E, (1996).
29. CLEO Collaboration, P. Avery *et al.*, Phys. Rev. Lett. 68, 1279 (1992).
30. CLEO Collaboration, J. Bartelt *et al.*, “*Measurement of the Two-Body D_s^+ Decays to $\eta\pi^+$, $\eta'\pi^+$, $\eta\rho^+$, and $\eta'\rho^+$* ”, ICHEP-96 PA05-114. Submitted paper to the 28th International Conference on High Energy

- Physics, Warsaw, (1996) The postscript version can be obtained at <http://w4.lns.cornell.edu/public/CONF/1996>
31. Ian Hinchliffe and Thomas A. Kaeding, “*Nonleptonic Two-Body Decays of D Mesons in Broken SU(3)*”, LBL-35892, (1995).
 32. F. Buccella, M. Lusignoli, and A. Pugliese, “*Charm nonleptonic decays and final state interactions*”, [hep-ph/9601343](#).
 33. M. Bauer *et al.*, Z. Phys. C - Particles and Fields **34**, 103 (1987).
 34. CLEO Collaboration, “*Observation of the Decay $D_s^+ \rightarrow \omega\pi^+$* ”, submitted to Phys. Rev. Lett.
 35. E691 Collaboration, J. C. Anjos *et al.*, Phys. Rev. Lett. **62**, 125 (1989), Phys. Lett. **B223**, 267 (1989).
 36. H. Lipkin, “*Symmetry, Topology, and Helicity in $D_s^+ \rightarrow \omega\pi^+$ and $D_s^+ \rightarrow \rho^0\pi^+$* ”, published in the Proc. of 1989 Int. Symp. on Heavy Quark Physics, Ithaca, N.Y., Jun 13-17, 1989.
 37. H. Lipkin, “*A Flavor-topology Classification of Diagrams in B and D Decays*”, (1992), unpublished; F.E. Close and H. Lipkin, “*Final State Interactions, Resonances and CP Violation in D and B Exclusive Decays*”, [hep-ph/9607349](#).
 38. F. Buccella, M. Lusignoli, G. Miele, A. Pugliese, and P. Santorelli, “*Nonleptonic weak decays of charmed mesons*”, [hep-ph/9411286](#).
 39. P. Ball, J.-M. Frère, and M. Tytgat, “*Phenomenological Evidence for the Gluon Content of the η and η'* ”, [hep-ph/9508359](#).